Julian-Valenzuela, J.; Coego Gonzalez, A.; Lozano Juste, J.; Lechner, E.; Wu, Q.; Zhang, X.; Merilo, E.... (2019). The MATH-BTB BPM3 and BPM5 subunits of Cullin3-RING E3 ubiquitin ligases target PP2CA and other clade A PP2Cs for degradation. Proceedings of the National Academy of Sciences. 116(31):15725-15734. https://doi.org/10.1073/pnas.1908677116

The MATH-BTB BPM3 and BPM5 subunits of Cullin3-RING E3 ubiquitin ligases target PP2CA and other clade A PP2Cs for degradation

Jose Julian[#1], Alberto Coego[#1], Jorge Lozano-Juste[1], Esther Lechner[2], Qian Wu[3,4], Xu Zhang[3,5], Ebe Merilo[6], Borja Belda-Palazon[1], Sang-Youl Park[7], Sean R. Cutler[7], Chengcai An[3], Pascal Genschik[2] and Pedro L. Rodriguez[*1]

[1]Instituto de Biología Molecular y Celular de Plantas, Consejo Superior de Investigaciones Cientificas-Universidad Politecnica de Valencia, ES-46022 Valencia, Spain.

[2]Institut de Biologie Moleculaire des Plantes, Centre National de la Recherche Scientifique, Université de Strasbourg, 67084 Strasbourg, France

[3]The State Key Laboratory of Protein and Plant Gene research, College of Life Sciences, School of Agriculture Science, Peking University, Beijing, 100871, P. R. China.

[4]Department of Plant Molecular Biology. Biophore Building, University of Lausanne, 1015 Lausanne, Switzerland

[5]Department of Molecular Biology and Institute of Genetics and Genomics, University of Geneva, 30 quai Ernest-Ansermet, 1211 Geneva, Switzerland

[6]Institute of Technology, University of Tartu, Nooruse 1, 50411 Tartu, Estonia

[7]Department of Botany and Plant Sciences, Institute of Integrative Genome Biology, University of California, Riverside, California 92521, United States.

[#]These authors contributed equally to this work and should be considered co-first author.

[*]Address correspondence to Pedro L. Rodriguez prodriguez@ibmcp.upv.es

Instituto de Biología Molecular y Celular de Plantas (CSIC-UPV)

Avd de los Naranjos s/n. Edificio CPI, 8E. Valencia 46022. Spain

Phone: +34 963877860

coc5af5a0f564b60

Abstract

Early abscisic acid signaling involves degradation of clade A protein phosphatases type 2C (PP2Cs) as a complementary mechanism to PYR/PYL/RCAR-mediated inhibition of PP2C activity. At later steps, ABA induces upregulation of *PP2C* transcripts and protein levels as a negative feedback mechanism. Therefore, resetting of ABA signaling also requires PP2C degradation to avoid excessive ABA-induced accumulation of PP2Cs. It has been demonstrated that ABA induces the degradation of existing ABI1 and PP2CA through the PUB12/13 and RGLG1/5 E3 ligases, respectively. However, other unidentified E3 ligases are predicted to regulate protein stability of clade A PP2Cs as well. In this work we identified BTB/POZ AND MATH DOMAIN proteins (BPMs), substrate adaptors of the multimeric cullin3 (CUL3)-RING based E3 ligases (CRL3s), as PP2CA-interacting proteins. BPM3 and BPM5 interact in the nucleus with PP2CA as well as with ABI1, ABI2 and HAB1. BPM3 and BPM5 accelerate the turnover of PP2Cs in an ABA-dependent manner and their overexpression leads to enhanced ABA sensitivity, whereas *bpm3 bpm5* plants show increased accumulation of PP2CA, ABI1 and HAB1, which leads to global diminished ABA sensitivity. Using biochemical and genetic assays we demonstrated that ubiquitination of PP2CA depends on BPM function. Given the formation of receptor-ABA-phosphatase ternary complexes is markedly affected by the abundance of protein components and ABA concentration, we reveal that BPMs and multimeric CRL3 E3 ligases are important modulators of PP2C co-receptor levels to regulate early ABA signaling as well as the later desensitizing-resetting steps.

Significance statement

Relief of repression imposed by negative regulators is a crucial mechanism for plant hormone signaling. Clade A PP2Cs are key negative regulators of ABA signaling that are inhibited by ABA receptors. Degradation of PP2Cs is a complementary mechanism to PYR/PYL/RCAR-mediated ABA-dependent inhibition of PP2Cs. We reveal that BTB/POZ AND MATH DOMAIN proteins (BPMs), substrate adaptors of the multimeric cullin3 (CUL3)-RING based E3 ligases (CRL3s), target PP2Cs for degradation. BPM-dependent degradation of

PP2Cs is required for ABA-induced stomatal closure, to counteract ABA-induced accumulation of PP2Cs and to reset resting phosphatase levels that allow efficient ABA signaling. Therefore, BPM-mediated proteolysis of transcription factors and clade A PP2Cs emerges as a general mechanism to regulate stress response and ABA signaling.

\body

Introduction

The plant hormone abscisic acid (ABA) regulates many key processes in plants, including seed germination and development and various biotic and abiotic stress responses (1, 2). The ABA signaling pathway is initiated by ABA perception through PYRABACTIN RESISTANCE1 (PYR1)/PYR1-LIKE (PYL)/REGULATORY COMPONENTS OF ABA RECEPTORS (RCAR) family of proteins (3-6). This is followed by interaction with and inactivation of clade A protein phosphatases type 2C (PP2Cs), such as ABA INSENSITIVE 1 (ABI1) and ABI2, HYPERSENSITIVE TO ABA (HAB1) and HAB2, and PROTEIN PHOSPHATASE 2CA/ABA-HYPERSENSITIVE GERMINATION 3 (PP2CA/AHG3), thereby relieving their inhibition on three ABA-activated SNF1-related protein kinases (SnRK2s), i.e. SnRK2.2/D, 2.3/I and 2.6/E/OST1 (7, 8). Then these SnRK2s activate downstream signaling by phosphorylation of numerous targets, including ABA-responsive transcription factors (9-11), the chromatin-remodeling ATPase BRAHMA (12), ion and water channels (13-15) and other mediators/effectors involved in ABA signaling and action (16, 17). Transcription of some PYR/PYL/RCARs is repressed whereas that of PP2Cs is stimulated in response to ABA (5, 18), indicating there exists a negative feedback transcriptional mechanism to modulate ABA signaling by controlling transcript levels of core elements. Recently, it has been discovered that degradation of PP2Cs is a complementary mechanism to PYR/PYL/RCAR-mediated inhibition of PP2C activity (19-21).

The ubiquitin (Ub)-proteasome system (UPS) plays a crucial role in plant hormone signaling (22). Ubiquitination, in addition to commit proteins to degradation by the 26S proteasome, also influences proteasome-independent cellular roles (23, 24). Through an ATP-dependent conjugating cascade, free

Ubs are attached to intracellular targets via E1, E2 and E3 Ub ligase enzymes. In particular, E3 Ub ligases, as the last component of the Ub conjugation cascade, are responsible for specific recognition of the many cellular proteins that are ubiquitinated. In *Arabidopsis* more than 1500 genes encode putative E3 subunits, being a major part represented by the almost 700 F-box proteins from the multimeric E3 ligases and in second place by the more than 500 monomeric RING/U-box E3 ligases. Among the multimeric E3 ligases, the cullin-RING based E3 ligases (CRLs) are the best characterized to date (25). In Arabidopsis, CRLs based on cullin1-, cullin3- (CUL3) and cullin 4-scaffolds are the best known and play critical roles for hormone signaling (25, 26).

Recently, studies that address the turnover of core ABA signaling components have been published (19-21, 27-32). Regarding the turnover of clade A PP2Cs, in the case of ABI1, it has been demonstrated that ABA induces degradation of this PP2C through PUB12/13 E3 ligases (19). PUB13-mediated ABI1 ubiquitination in presence of PYR1 was strictly dependent on ABA, whereas in presence of monomeric receptors ABA increased ABI1 ubiquitination level (19). PP2CA is another key negative regulator of ABA signaling (14, 33-37). Recently we demonstrated that the RGLG1 and RGLG5 RING-type E3 ubiquitin ligases relieve PP2C blockade of ABA signaling by mediating PP2CA protein degradation, which is enhanced by ABA (20, 21). However, experiments with double *rglg1 rglg5* mutants indicated that additional unidentified E3s contribute to regulation of PP2CA levels (20). Thus, during the course of our proteomic studies aimed to identify PP2CA interacting proteins, in addition to RGLG1 and RGLG5, we also identified BTB/POZ AND MATH DOMAIN proteins (BPMs), substrate adaptors of the multimeric CUL3-RING based E3 ligases (CRL3s). BPMs belong to a six-member protein family in Arabidopsis, BPM1 to 6 (38), and BPM3, BPM4 and BPM5 were identified after mass spectrometry analysis of PP2CA-coimmunoprecipitated proteins.

BPMs contain two conserved domains, the MATH and the BTB/POZ domain, the former acting as substrate receptor and the latter binding CUL3 (39). CRL3 complexes also contain the RING-BOX (RBX) adaptor for E2 binding and a variety of receptors recognizing specific substrates for ubiquitination (38, 39). The MATH domain functions as the recognition site for

various substrates of the BPM-CUL3 E3 ligase (hereinafter called $CRL3^{BPM}$) (38, 40-42). For instance, studies performed with the MATH-BTB SPOP protein (BPM ortholog in humans) to determine MATH-substrate interactions have revealed that the MATH domain can recognize a consensus peptide sequence in different targets, e.g. the phosphatase Puc, transcription factor Ci and histone macroH2A (40). In *Arabidopsis*, the MATH domain of BPM3 interacts with the leucine zipper (ZIP) domain of AtHB6, a transcription factor from the class I homeobox-ZIP that negatively regulates ABA responses and is a target of the clade A PP2C ABI1 (38). Reducing $CRL3^{BPM}$ function enhances the ABA-insensitive phenotype of lines overexpressing AtHB6, which indicates that $CRL3^{BPM}$ function positively regulates ABA signaling (38). Recently, the DREB2A transcription factor (TF), a key factor mediating transcriptional response to drought and heat stresses, has been identified as another target of BPMs and it seems that various TFs harbor BPM recognition motifs, which implies a wider role of BPM-dependent proteolysis in stress response (43). Interestingly, our results identify additional targets of BPMs and indicate that BPM3 and BPM5 promote proteasomal degradation of clade A PP2Cs through $CRL3^{BPM}$ complexes, which counteracts the PP2C accumulation induced in response to ABA to desensitize ABA signaling.

Results

Identification of BPMs as interacting proteins of PP2CA

We performed coimmunoprecipitation (coIP) coupled with liquid chromatography-tandem mass spectrometry (LC-MS/MS) to identify proteins that coimmunoprecipitate with FLAG-tagged PP2CA expressed in Arabidopsis. In protein extracts obtained from 2-week-old seedlings after 30 h of treatment with the proteasome inhibitor MG132 and 6h with ABA, but not in mock-treated samples, we found that native BPM3, BPM4 and BPM5 proteins co-immunoprecipitated with FLAG-PP2CA (Fig. 1A; SI appendix, Table S1 and S2). The additional identification of RGLG1 during LC-MS/MS analysis, which has been reported as a PP2CA-interacting protein (20), validates this screening system (SI appendix, Table S2). We concentrated further work on BPM3 and BPM5 because we recovered more peptides from these proteins compared to BPM4 in additional experiments (SI Appendix, Table S2). First of all, we

performed bimolecular fluorescence complementation (BiFC) assays to analyze whether PP2CA interacts with BPM3 and BMP5 in planta (Fig. 1B and C). We found that PP2CA, as well as the clade A PP2Cs HAB1, ABI1 and ABI2, show nuclear interaction with both BPM3 and BPM5, which are localized *per se* in the nucleus (Fig. 1B and C; SI Appendix, Fig. S1A). By contrast, YFP^C-BPM3 or YFP^C-BPM5 does not interact with YFP^N-empty nor YFP^N-PYL8, neither YFP^N-PP2C fusions interact with YFP^C-OST1Δ280 (8) (Fig. 1C; SI Appendix, Fig. S1B and S2). Since the MATH domain is presumed to contain the substrate recognition module of CRL3s, we tested whether it might recognize PP2Cs. To this end we split BPM3 in two regions, the N-terminal containing the MATH domain (residues 1-175) and the C-terminal containing the BTB domain (residues 176-408). As expected, only the MATH region of BPM3 showed interaction with PP2CA (SI Appendix, Fig. S1C). Finally, we also tested whether the N-terminal region of PP2CA, which corresponds to the most variable part of clade A PP2Cs, was required for the interaction with BPMs. To this end, ΔNPP2CA (lacking amino acid residues 1-99) was assayed in BiFC and we found that the catalytic core of PP2CA was sufficient for interaction with both BPM3 and BPM5 in nuclear speckles, whose shape differs in BPM3 compared to BPM5 (SI Appendix, Fig. S1D; see also Fig. 1B and 1C). Finally, we also verified that YFP^N- and YFP^C-fusion proteins were correctly expressed (SI Appendix, Fig. S1E). The reconstituted YFP signal in BiFC experiments described above was quantified from 10 randomly chosen regions of infiltrated leaves by Image J software and the arbitrary units of fluorescence are indicated in numbers (SI Appendix, Fig. S2).

To validate the BiFC interactions observed for PP2CA and HAB1 with BPMs, we performed a split-luciferase (split-LUC) complementation assay in *N. benthamiana* leaves (Figure 1D). In contrast to BiFC assays, the restoration of luciferase activity upon protein-protein interaction of the candidate proteins is reversible. The coexpression of PP2CA-nLUC and BPM3-cLUC or BPM5-cLUC reconstituted luciferase activity as well as co-expression of HAB1-nLUC and BPM3-cLUC or BPM5-cLUC (Figure 1D), whereas the corresponding negative controls did not (Figure 1D). Finally, we performed yeast two-hybrid (Y2H) interaction assays of the PP2CA, ABI1 and HAB1 phosphatases fused to the

Gal4 activation domain (AD) with either BPM3 or BPM5 fused to the Gal4 DNA binding domain (BD). As a result, we could confirm the in planta interactions observed above using Y2H growth assays (Figure 1E).

Next we performed pull-down assays with His-tagged PP2CA and other clade A PP2Cs, such as HAB1, ABI1 and ABI2, using GST-BPM5 as bait because GST-BPM3 was poorly soluble and tends to unspecific precipitation. We found that all the PP2Cs tested interacted with BPM5 (Fig. 2A). The ΔNPP2CA version also interacted with BPM5 in the pull-down assay, which confirms that the catalytic core of PP2CA can be recognized by BPM5 (Fig. 2B; SI Appendix, Fig. S1D). We also confirmed that the MATH domain of BPM3 and BPM5 was able to interact with GST-PP2CA but not with GST (Fig. 2C). Finally, we performed coIP assays of PP2CA-GFP and either HA-BPM3 or HA-BPM5 coexpressed in *N. benthamiana* leaf cells. These assays revealed that PP2CA-GFP but not GFP co-immunoprecipitated with either BPM3 or BPM5 (Fig. 2D). Similar results were obtained for GFP-ABI1 and GFP-HAB1 (Fig. 2D), although we noticed that co-expression of the PP2Cs with BPMs reduced PP2C protein levels (SI Appendix, Fig. S3A).

BPM3 and BPM5 promote degradation of clade A PP2Cs in vivo

Once we confirmed the interaction of BPM3 and BPM5 with clade A PP2Cs, co-infiltration experiments in *N. benthamiana* were performed to test whether they promote degradation of PP2CA (44). Increasing amounts of the Agrobacterium that drives expression of the BPM subunit of the CRL3 E3 ligase were co-infiltrated with Agrobacteria encoding the construct that expresses PP2CA-GFP. Samples were collected for detection of both protein and RNA levels of transfected constructs (Fig. 3A; SI Appendix, Fig. S3B). Increasing amounts of BPM3 or BPM5 led to decreased levels of PP2CA, whereas the internal RFP control was not significantly affected by increasing the amount of BPMs. Interestingly, at the 4:1 ratio (PP2CA:BPM), the addition of ABA enhanced the degradation of PP2CA by both BPM3 and BPM5. When the expression of BPM5 was higher (4:4 ratio), the enhanced degradation of PP2CA precluded the observation of any effect due to ABA addition (Fig. 3A, right panel). Co-expression of BPM3 or BPM5 with GFP-ABI1 or GFP-HAB1 also led to

decreased levels of the PP2Cs compared to expression in the absence of the BPMs (SI Appendix, Fig. S3A).

We generated Arabidopsis lines that overexpress either HA-tagged BPM3 or BPM5 (SI Appendix, Fig. S4A) and analyzed endogenous PP2CA levels in root tissue to avoid masking of the PP2CA signal by the very close RBC large subunit (Fig. 3B). Additionally, high induction by ABA of PP2CA, HAB1 and ABI1 proteins was detected in roots (Fig. 3B and 3D) (45). Using specific antibodies to detect endogenous PP2CA, we found lower PP2CA levels in BPM3 and BPM5 OE lines compared to wild type, which was apparent both in mock- and ABA-treated samples (Fig. 3B). Plants of two BPM5 OE lines grown in soil under green house conditions also showed reduced accumulation of PP2CA in leaves after spraying with ABA (Fig. 3C). Conversely, in the loss-of-function *bpm3 bpm5* double mutant (described in SI Appendix, Fig. S4B) more PP2CA accumulated after ABA treatment compared to wild type (Fig. 3D). Other PP2Cs that are induced by ABA and play a key role for ABA signaling, such as HAB1 and ABI1, also accumulated more in *bpm3 bpm5* than in wild type (Fig. 3D). Analysis of the specificity of the HAB1 antibody is provided in SI Appendix, Fig. S5. Finally, after induction of PP2CA by ABA treatment and washing ABA, we performed a time course of the protein in the presence of CHX (Fig. 3E). Degradation of PP2CA was slower in *bpm3 bpm5* compared to wild type; however at 6h still ~60% PP2CA was degraded, indicating that additional E3s (such as RGLG1/5) or non-26S proteasome pathways also are involved in PP2CA degradation (Fig. 3E) (20, 24).

BPM3 and BMP5 gain-of-function leads to enhanced sensitivity to ABA whereas *bpm3 bpm5* shows reduced ABA sensitivity

BPMs belong to a six-member family and the phenotypic analysis of *amiR-bpm* plants impaired in transcript expression of *BPM1*, *4*, *5* and *6* revealed that BPMs are required for normal plant development (38). Leaf shape, leaf size and stem elongation were affected in these lines, as well as the overall stature of the plants, and a severe phenotype in flower development and reduced pollen viability was also observed. In contrast, single *bpm* knockouts did not show these phenotypes (38). Taking into account the possible functional redundancy of *BPM* genes, we started our ABA-response phenotypic analysis using

overexpressing (OE) lines of either BPM3 or BPM5 (Fig. 4A-D). BPM3 and BPM5 OE lines showed enhanced ABA-mediated inhibition of seed germination, seedling establishment and root growth (Fig. 4A-C). Because ABA also plays a critical role in regulating stomatal aperture and water loss, we measured water loss in 21-d-old plants OE BPM3 and BPM5. We found that detached leaves of both BPM3 and BPM5 OE plants showed reduced water loss compared with the wild type (Fig. 4D). Additionally, BPM5 OE lines showed enhanced drought resistance under greenhouse conditions compared with the wild type (SI Appendix, Fig. S6).

Conversely, we could confirm that detached leaves of *amiR-bpm* plants showed higher water-loss and *amiR-bpm* plants displayed lower leaf temperature compared to wild type (Fig. 4E; see below Figure 5C) (38). These data suggest that ABA-induced stomatal closure might be impaired in *amiR-bpm* plants. Well-watered *amiR-bpm* and Col-0 plants had similar pre-ABA stomatal conductances (G_{st}) and both lines showed ABA-induced stomatal closure (Fig 4F). However, after ABA treatment G_{st} of well-watered *amiR-bpm* plants was significantly higher compared to Col-0, indicating that ABA-induced reduction of G_{st} was impaired in *amiR-bpm* plants (Fig. 4F). We then grew plants under soil water deficit and found the same results – no difference in pre-ABA G_{st} and reduced ABA-response of *amiR-bpm* (Fig. 4G). ABA induced stomatal closure was not significantly affected in *bpm3 bpm5*, in contrast to *amiR-bpm* plants, which suggests certain functional redundancy of the BPM family in the control of stomatal aperture (Fig. 4H)..

Given the growth and developmental defects of *amiR-bpm* plants, we conducted further phenotypic analysis with the *bpm3 bpm5* double mutant, which accumulates more PP2Cs than wild type in root tissue (Fig. 3D). *bpm3 bpm5* showed reduced sensitivity to ABA-mediated inhibition of seedling establishment and root-growth (Fig. 5A and B). The *bpm3 bpm5* mutant accumulates more PP2CA, which is a phosphatase that strongly blocks ABA signaling during germination and early growth (34, 35). Since PP2CA plays a predominant role at this stage and *pp2ca-1* shows the strongest ABA hypersensitivity in seed germination assays compared to other loss-of-function *pp2c* mutants (34-36), we generated a *pp2ca-1 bpm3 bpm5* triple mutant for

epistatic analysis. ABA-mediated inhibition of seedling establishment in the triple mutant became similar to that of *pp2ca-1*; therefore *pp2ca-1* was epistatic to *bpm3 bpm5* (Figure 5A). Transpiration was monitored using infrared thermography and we found that *bpm3 bpm5* showed lower leaf temperature than wild type, whereas *amiR-bpm* plants showed lower leaf temperature than *bpm3 bpm5* (Fig. 5C). Using RT-qPCR analysis, we found lower expression of ABA-responsive genes at endogenous ABA levels in *bpm3 bpm5* compared to wild type (Fig. 5D). We also analyzed induction of the ABA-responsive promoter *RD29B* after ABA treatment by using transfection of wild type or *bpm3 bpm5* protoplasts. We measured ABA-induced luciferase (LUC) expression driven by p*RD29B* and we found reduced expression in *bpm3 bpm5* compared to Col-0, both when ABF2 or ABF2+OST1 effector plasmids were transfected (Fig. 5E).

In vivo ubiquitination of PP2CA depends on BPM proteins

Transient expression of PP2CA-GFP in *N. benthamiana* and β-estradiol-inducible expression of Flag-Ub was performed to detect in vivo ubiquitination of PP2CA (Fig. 6A). To this end we constructed a β-estradiol-inducible Flag-Ub vector that was co-expressed in *N. benthamiana* with HA-BPM3 and PP2CA-GFP. Two days after agroinfiltration 1.5 cm disk samples were collected and incubated for 16 h in 100 μM β-estradiol to induce expression of Flag-Ub and label ubiquitinated PP2CA. Protein extracts were prepared from the disk samples, PP2CA-GFP was immunoprecipitated using anti-GFP and analyzed by immunoblotting with four different antibodies (Fig. 6A). When PP2CA-GFP was co-expressed with HA-BPM3 and β-estradiol-induced Flag-Ub, PP2CA was mostly shifted to the mono-ubiquitinated form, in contrast to mock-treated samples (Fig. 6A, arrows indicate different mobility of UbPP2CA-GFP and PP2CA-GFP). HA-BPM3 co-immunoprecipitated with PP2CA-GFP (Fig. 6A, anti-HA panel), which was previously observed in coIP experiments (Fig. 2D). Using anti-FLAG antibody, we could detect incorporation of Flag-Ub in immunoprecipitated PP2CA-GFP, which was confirmed using anti-Ub antibody. In mock-treated samples, some ubiquitinated PP2CA-GFP could be detected using anti-Ub antibody (but not with anti-Flag), which likely corresponds to protein ubiquitinated by the endogenous endowment of *N. benthamiana* cells.

Upon longer exposition of the film, polyubiquitinated forms of PP2CA could be observed (right panel, Fig. 6A)

We also investigated the ubiquitination of endogenous PP2CA in Arabidopsis wild type, *bpm3 bpm5* and *amiR-bpm* plants. We prepared root protein extracts from 10-d-old seedlings that were incubated for 3 h with MG132 and ABA. Next, total proteins were incubated with Ub-binding p62 agarose or with agarose lacking p62 (negative control). Immunoblotting analysis using anti-PP2CA antibodies allowed the detection of endogenous PP2CA and its mono-ubiquitinated form (Fig. 6B). More non-ubiquitinated PP2CA accumulated in *bpm3 bpm5* and *amiR-bpm* plants compared to Col-0 wild type (Fig. 6C, left); however, after pull-down with p62 agarose more ubiquitinated PP2CA was recovered in Col-0 samples than in *bpm3 bpm5* and *amiR-bpm* (Fig. 6B and C, right). Taken together, these results confirm that ubiquitination of PP2CA depends on BPM function.

Discussion

Both early and late steps of ABA signaling require a mechanism that modulates activity and protein levels of clade A PP2Cs because they are core negative regulators of the pathway. This is achieved through regulation of PP2C activity, transcripts and protein levels (3-5, 19, 20, 45). For instance, the strong activation of ABA signaling also leads to transcriptional upregulation of clade A PP2Cs as a negative feedback mechanism (5). This is accompanied by transcriptional downregulation of some ABA receptors (5, 18), which combined with increased PP2C levels should relieve the inhibition of PP2C activity carried out by ABA receptors. Therefore, a desensitizing mechanism based on adjusting PP2C co-receptor and ABA receptor stoichiometry follows ABA signaling and, eventually, a mechanism involving degradation of PP2Cs is required to reset resting PP2C levels in the absence of stress. In this work we report that BPM3 and BPM5, which are substrate adaptors of the multimeric CRL3 E3 ligases, mediate recognition and degradation of key phosphatases for ABA signaling. Thus, using specific antibodies for PP2CA, HAB1 and ABI1, we could demonstrate that accumulation of these phosphatases is increased in the *bpm3 bpm5* mutant (Fig. 3D). On the other hand, we found that increasing

amounts of BPM3 and BPM5 lead to reduced levels of PP2CA and enhanced sensitivity to ABA compared to wild-type Col-0 (Fig. 3A-C and Fig. 4A-C).

Transient expression experiments in *N. benthamiana* revealed that ABA enhances BPM3/5-mediated degradation of PP2CA, in agreement with previous results for PUB12-mediated degradation of ABI1 or RGLG1-mediated degradation of PP2CA (19-21). Therefore, these data suggest that at resting ABA levels, PP2C protein levels remain sufficient to block ABA signaling because interaction with E3 ligases is dependent on ABA concentration. When ABA levels increase in response to stress, biochemical inhibition of PP2C activity by ABA-bound PYLs will lead to activation of ABA signaling and plant protection. In a short-term, this is complemented by the enhanced degradation of PP2Cs by different E3 ligases, i.e. U-box type, RING type and multimeric CRL3 type (19, 20, this work). Thus, these E3 ligases can facilitate ABA signaling at early steps. We also propose that at later steps E3 ligases play an important role to prevent excessive accumulation of PP2Cs and enable the resetting of ABA signaling. The finding of several E3 ligases that regulate PP2C levels is reminiscent of the team tagging cooperation described in humans to regulate substrate ubiquitination by different E3-E3 pairs (46). Thus, exquisite regulation of substrate ubiquitination can be achieved by combination of different E3s in mammals, which is an interesting issue to be investigated in the plant field.

Recent reports have revealed that levels of ABA receptors are regulated in different subcellular compartments (27, 28), and similar mechanisms might be used with PP2C co-receptors. For instance, the subcellular localization of the PUB12-ABI1 interaction has not been reported yet, but taking into account the membrane recruitment of PUB12 by Flagellin-sensing 2 (FLS2) (47), it is possible that PUB12-ABI1 interact in the proximity of plasma membrane, where PP2Cs regulate both ABA signaling and ABA effectors (13, 14, 48, 49). Alternatively, unidentified membrane-linked E3 ligases might regulate PP2Cs in an analogous manner to RSL1-dependent ubiquitination of ABA receptors (27, 30). BPM3 and BPM5 are nuclear proteins and accordingly, interact with PP2CA, HAB1 and ABI1 in the nucleus of plant cells. Nuclear accumulation of abi1^{Gly180Asp} blocks ABA signaling (50), likely because PP2Cs regulate critical

nuclear components of the ABA signaling pathway, such as SnRK2s, CDPKs, ABRE-binding transcription factors, and the chromatin remodeling ATPase BRAHMA (7, 8, 12, 51, 52). The nuclear interaction of BPM3/5 with clade A PP2Cs reveals that half-life regulation of the PP2C nuclear pool is required for ABA signaling.

Materials and Methods

Plant Material and growth conditions

Arabidopsis thaliana plants were grown as described (53). The *bpm3* and *bpm5* T-DNA insertion lines, WiscDsLox239E10 and SALK_038471C, respectively, were obtained from the Nottingham *Arabidopsis* Stock Centre (http://nasc.nott.ac.uk). To confirm and identify homozygous T-DNA individuals, seedlings of each insertion line were grown individually and DNA from each plant was extracted and submitted to PCR-mediated genotyping using the primers described in SI appendix, Table S3. The *bpm3 bpm5* double mutant was generated by crossing and genotyping of F2 individuals. The *bpm3 bpm5* double mutant was crossed with pp2ca-1 to generate the bpm3 bpm5 pp2ca-1 triple mutant, which was genotyped using the primers described in SI appendix, Table S3. The pAlligator2-*35S:HA-BPM3* and pAlligator2-*35S:HA-BPM5* constructs were transferred to *Agrobacterium tumefaciens* C58C1 (pGV2260) (54) by electroporation and used to transform Columbia wild type plants by the floral dip method (55). T1 transgenic seeds were selected based on seed GFP fluorescence and sowed in soil to obtain the T2 generation. Homozygous T3 progeny was used for further studies and expression of HA-tagged protein was verified by immunoblot analysis using anti-HA-HRP.

Constructs

The ORF of BPM3 or BPM5 was amplified by PCR and cloned into pENTR221 (38). The pENTR221-BPM3/BPM5 constructs were recombined by LR reaction into pAlligator2, to generate 35S:HA-BPM3 or 35S:HA-BPM5 constructs, or into pMDC43 to generate 35S:GFP-BPM3 or 35S:GFP-BPM5 constructs. BPM3 and BPM5 ORFs were recombined by LR reaction into pYFPC43 for BIFC assays, whereas PP2Cs were recombined into pYFPN43. BPM3 was split into the BTB and MATH domains using PCR and the primers described in SI appendix, Table

S3, in order to generate pCR8-BTB3 and pCR8-MATH3. These constructs and pCR8-MATH5 were recombined by LR reaction into pYFPC43 for BIFC assays.

Transient protein expression in *N. benthamiana*

Agrobacterium infiltration of tobacco leaves was performed basically as described by (56). To investigate the interaction of BPM3 and BPM5 with PP2Cs in planta, we used the pYFP^{N}43 and pYFP^{C}43 vectors for BiFC assays (57). The different binary vectors where introduced into *Agrobacterium tumefaciens* C58C1 (pGV2260) by electroporation and transformed cells were selected in LB plates supplemented with kanamycin (50 μg/ml). Then, they were grown in liquid LB medium to late exponential phase and cells were harvested by centrifugation and resuspended in 10 mM morpholinoethanesulphonic (MES) acid-KOH pH 5.6 containing 10 mM MgCl2 and 150 mM acetosyringone to an OD600 nm of 1. These cells were mixed with an equal volume of *Agrobacterium* C58C1 (pCH32 35S:p19) expressing the silencing suppressor p19 of tomato bushy stunt virus so that the final density of *Agrobacterium* solution was about 1. Bacteria were incubated for 3 h at room temperature and then injected into young fully expanded leaves of 4-week-old *Nicotiana benthamiana* plants. Leaves were examined 48-72 h after infiltration using confocal laser scanning microscopy.

***In vivo* protein degradation assays**

Protein degradation assays were performed as described (44) with small modifications**.** For *in vivo* protein degradation experiments, *A. tumefaciens* cultures containing constructs that express HA-BPM3 or HA-BPM5, PP2CA-GFP and the silencing suppressor p19 were co-infiltrated at different ratios in tobacco leaves. Three days after infiltration, samples were collected, ground in liquid nitrogen and immediately placed in lysis buffer (50 mM Tris-HCl pH 8.0, 150 mM NaCl, 1% Triton X-100, 3 mM DTT, 50 μM MG-132 and protease inhibitor cocktail) on ice for protein extraction. Homogenates were cleared by centrifugation at 12000 g, 4ºC for 15 min, and supernatants were used for protein immunoblot analysis. Samples were also collected for *Actin* and *PP2CA* mRNA analyses to ensure equal amounts of *PP2CA* transcript were expressed

in different co-infiltrations. Similar methods were used for the analysis of GFP-ABI1 and GFP-HAB1 degradation promoted by HA-BPM3 or HA-BPM5.

Split luciferase (LUC) complementation assay

The coding sequences of PP2CA and HAB1 lacking the stop codon were amplified by PCR and cloned into pCR8/GW. Then they were recombined by LR reaction into pDEST-GWnLUC (58). Coding sequences of BPM3 or BPM5 lacking the stop codon were recombined by LR reaction into pDEST-GWcLUC (58). Split-LUC complementation assay was performed by transient expression in leaves of *N. benthamiana* by agroinfiltration as described above but in this case the final density of the *Agrobacterium* solution was 0.1. MG132 (50 μM) was applied into the infiltrated region 12 h before inspection, which was performed 60 h after infiltration. To this end, leaves co-expressing different constructs were examined for LUC activity by applying 1 mM D-luciferin and placed in the dark for 5 min before imaging. LUC complementation was observed with a CCD imaging system (LAS3000, Fujifilm) using 10 min exposures.

For quantification of LUC activity, leaf samples were collected, ground in liquid nitrogen and immediately placed in lysis buffer (50 mM Tris-HCl pH 8.0, 150 mM NaCl, 1% Triton X-100, 3 mM DTT, 50 μM MG-132 and protease inhibitor cocktail) in ice for protein extraction. Homogenates were cleared by centrifugation at 12000 g, 4ºC for 15 min, and supernatants were used to quantify luminescence activity by the Luciferase Assay System (Promega, E1500) using 10 μg of protein. Luminescence was analyzed using a Glomax Multi Detection System (Promega, E7071). In order to normalize LUC values, we co-infiltrated all leaves with a GUS expression vector (pEXP:GUS) (58) and GUS activity was analyzed using 4-methyl umbelliferyl glucuronide (MUG) as substrate and the above mentioned detection system.

Protein stability kinetics

Seedlings of Col-0 wt or bpm3 bpm5 were grown in liquid MS medium for 10 days, and then were supplemented with 50 μM ABA for 3h to induce expression of PP2CA. Next, ABA was washed, 50 μM CHX was added and root samples were harvested at 0, 1, 3 and 6 h. Total proteins were extracted by

homogenizing the seedlings in lysis buffer containing 50 mM Tris-HCl pH 8.0, 150 mM NaCl, 1% Triton X-100, 3 mM DTT, 50 µM MG-132 and protease inhibitor cocktail at 2:1 ratio (m/v). The concentration of total protein was determined by Bradford assays and equal amount of total proteins were mixed with 2× SDS loading buffer. Boiled samples were separated by SDS-PAGE gel electrophoresis and analyzed by immunoblot. The a-E2663 antibody was used to detect endogenous PP2CA. Actin was analyzed as a loading control using anti-Actin antibodies (Agrisera)

Protein extraction, analysis, immunodetection and co-immunoprecipitation (coIP)

Protein extracts for immunodetection experiments were prepared from *Arabidopsis* transgenic lines expressing HA-tagged BPM3 or BPM5. Material (~100 mg) for direct Western blot analysis was extracted in 2X Laemmli buffer (125 mM Tris-HCl pH 6.8, 4% SDS, 20% glycerol, 2% mercaptoethanol, 0.001% bromophenol blue), proteins were run in a 4-10% SDS-PAGE MiniProtean precast gel (BioRad) and analyzed by immunoblotting. Proteins were transferred onto Immobilon-P membranes (Millipore) and probed with anti-HA-peroxidase (Roche). Immunodetection of ubiquitylated proteins was performed using anti-Ub antibody (Ub P4D1:sc-8017, Santa Cruz Biotechnology). Antibodies were used to a 1:10000 dilution. Detection was performed using the ECL advance western blotting chemiluminiscent detection kit (GE Healthcare). Image capture was done using the image analyzer LAS3000 and quantification of the protein signal was done using Image Guache V4.0 software.

Co-IP experiments of PP2CA and BPM3/BPM5 were performed using agroinfiltration in *N. benthamiana.* Protein extracts were prepared in lysis buffer (50 mM Tris-HCl pH 8.0, 150 mM NaCl, 1% Triton X-100, 3mM DTT, 50 µM MG-132, protease inhibitor cocktail) from tobacco leaves 48 h after agroinfiltration with constructs to co-express GFP or PP2CA-GFP proteins and either HA-tagged BPM3 or BPM5. GFP or PP2CA-GFP proteins were immunoprecipitated using super-paramagnetic micro MACS beads coupled to monoclonal anti-GFP antibody according to the manufacturer´s instructions (Miltenyi Biotec). Purified immunocomplexes were eluted in Laemmli buffer, boiled and run in a 10% SDS-PAGE gel. Proteins immunoprecipitated with anti-

GFP antibody were transferred onto Immobilon-P membranes (Millipore) and probed with anti-HA-peroxidase to detect coIP of HA-tagged BPM3 or BPM5.

Pull-down assays

The construction of the plasmids, expression in BL21 (DE3) *E. coli* and purification of GST-BPM5 and GST-PP2CA was described in (38) and (59), respectively. BPM5 was induced with 0.5 mM IPTG for 4 h at 16ºC, whereas PP2CA with 1 mM IPTG over night at 16ºC. Purification of 6His-PP2CA, ΔNPP2CA, ABI1, ABI2 and HAB1 was described in (5) and (60). To generate 6His-MATH3 and 6His-MATH5, we cloned the corresponding *Nco*I-*EcoR*I fragment into pETM11 and induction of the proteins was done with 1 mM IPTG over night at 16ºC. For pull-down assays, glutathione agarose beads (ABT) containing approximately 50 μg of GST-BPM5 (38), GST-PP2CA (59) or GST were incubated with 50 μg of the indicated His-tagged proteins for 2 h at 4 ºC with constant rocking in 0.5 ml binding buffer (20 mM Tris-HCl pH 7.5, 200 mM NaCl, 1 mM EDTA, 0.5% Tween-20). After washing the beads with TBS, proteins that remained bound to the beads were eluted in hot 2X Laemmli buffer (125 mM Tris-HCl pH 6.8, 4% SDS, 20% glycerol, 2% mercaptoethanol, 0.001% bromophenol blue) and analysed by SDS-PAGE, followed by western blotting and immunodetection using anti His-tag monoclonal antibodies (Roche) or anti-GST antibodies (Sigma).

SI Appendix

Detailed description is provided in *SI Appendix* for antibodies, mass spectrometry (MS) analysis, seed germination and seedling establishment assays**,** root growth assay**,** RT-qPCR, *in vivo* ubiquitination assay of PP2CA-GFP in *N. benthamiana***,** affinity purification of ubiquitinated proteins using p62-agarose**,** water loss and drought stress experiments, gas exchange experiments, infrared thermography**,** protoplast transfection, confocal laser scanning microscopy (CLSM) and statistical analysis.

Acknowledgments

Work in P.L.R.'s laboratory was supported by the Ministerio de Ciencia, Innovacion y Universidades, Fondo Europeo de Desarrollo Regional and Consejo Superior de Investigaciones Cientificas through grants BIO2014-52537-R and BIO2017-82503-R. P.G. acknowledges support from the Agence Nationale de la Recherche LABEX, ANR-10-LABX-0036_NETRNA. B.B-P. was funded by Programa VALi+d GVA APOSTD/2017/039. J.J. was supported by a FPI contract from MICIU. J.L-J. was supported by a Juan de la Cierva contract from MINECO and by the Marie Skłodowska-Curie Action H2020-MSCA-IF-2015-707477. E.M. was supported by the Estonian Research Council (PUT1133). We acknowledge to Dr Pablo Tornero for the gift of the pDEST15 plasmid and anti-GST antibody.

References

1. Cutler SR, Rodriguez PL, Finkelstein RR, Abrams SR (2010) Abscisic acid: emergence of a core signaling network. *Annu Rev Plant Biol* **61:** 651-679.
2. Finkelstein R (2013) Abscisic Acid synthesis and response. *Arabidopsis Book* **11:** e0166.
3. Ma Y *et al.* (2009) Regulators of PP2C Phosphatase Activity Function as Abscisic Acid Sensors. *Science* **324:** 1064-1068.
4. Park SY *et al.* (2009) Abscisic Acid Inhibits Type 2C Protein Phosphatases via the PYR/PYL Family of START Proteins. *Science* **324:** 1068-1071.
5. Santiago J *et al.* (2009) Modulation of drought resistance by the abscisic acid receptor PYL5 through inhibition of clade A PP2Cs. *Plant J* **60:** 575-588.
6. Nishimura N *et al.* (2010) PYR/PYL/RCAR family members are major in-vivo ABI1 protein phosphatase 2C-interacting proteins in Arabidopsis. *Plant J* **61:** 290-299.
7. Umezawa T *et al.* (2009) Type 2C protein phosphatases directly regulate abscisic acid-activated protein kinases in Arabidopsis. *Proc Natl Acad Sci U S A* **106:** 17588-17593.
8. Vlad F *et al.* (2009) Protein phosphatases 2C regulate the activation of the Snf1-related kinase OST1 by abscisic acid in Arabidopsis. *Plant Cell* **21:** 3170-3184.
9. Fujii H *et al.* (2009) In vitro reconstitution of an abscisic acid signalling pathway. *Nature* **462:** 660-664.
10. Fujii H, Zhu JK (2009) Arabidopsis mutant deficient in 3 abscisic acid-activated protein kinases reveals critical roles in growth, reproduction, and stress. *Proc Natl Acad Sci U S A* **106:** 8380-8385.
11. Nakashima K *et al.* (2009) Three Arabidopsis SnRK2 protein kinases, SRK2D/SnRK2.2, SRK2E/SnRK2.6/OST1 and SRK2I/SnRK2.3, involved in ABA signaling are essential for the control of seed development and dormancy. *Plant Cell Physiol* **50:** 1345-1363.
12. Peirats-Llobet M *et al.* (2016) A Direct Link between Abscisic Acid Sensing and the Chromatin-Remodeling ATPase BRAHMA via Core ABA Signaling Pathway Components. *Mol Plant* **9:** 136-147.

13. Geiger D *et al.* (2009) Activity of guard cell anion channel SLAC1 is controlled by drought-stress signaling kinase-phosphatase pair. *Proc Natl Acad Sci U S A* **106:** 21425-21430.
14. Lee SC, Lan W, Buchanan BB, Luan S (2009) A protein kinase-phosphatase pair interacts with an ion channel to regulate ABA signaling in plant guard cells. *Proc Natl Acad Sci U S A* **106:** 21419-21424.
15. Grondin A *et al.* (2015) Aquaporins Contribute to ABA-Triggered Stomatal Closure through OST1-Mediated Phosphorylation. *Plant Cell* **27:** 1945-1954.
16. Umezawa T *et al.* (2013) Genetics and phosphoproteomics reveal a protein phosphorylation network in the abscisic acid signaling pathway in Arabidopsis thaliana. *Sci Signal* **6:** rs8.
17. Wang P *et al.* (2013) Quantitative phosphoproteomics identifies SnRK2 protein kinase substrates and reveals the effectors of abscisic acid action. *Proc Natl Acad Sci U S A* **110:** 11205-11210.
18. Szostkiewicz I *et al.* (2010) Closely related receptor complexes differ in their ABA selectivity and sensitivity. *Plant J* **61:** 25-35.
19. Kong L *et al.* (2015) Degradation of the ABA co-receptor ABI1 by PUB12/13 U-box E3 ligases. *Nat Commun* **6:** 8630.
20. Wu Q *et al.* (2016) Ubiquitin Ligases RGLG1 and RGLG5 Regulate Abscisic Acid Signaling by Controlling the Turnover of Phosphatase PP2CA. *Plant Cell* **28:**2178-2196
21. Belda-Palazon B et al. (2019). ABA inhibits myristoylation and induces shuttling of the RGLG1 E3 ligase to promote nuclear degradation of PP2CA. *Plant J* doi10.1111/tpj.14274
22. Santner A, Estelle M (2009) Recent advances and emerging trends in plant hormone signalling. *Nature* **459:** 1071-1078.
23. Romero-Barrios N, Vert G (2018) Proteasome-independent functions of lysine-63 polyubiquitination in plants. *New Phytol* **217:** 995-1011.
24. Yu F, Xie Q (2017) Non-26S Proteasome Endomembrane Trafficking Pathways in ABA Signaling. *Trends Plant Sci* **22:** 976-985.
25. Hua Z, Vierstra RD (2011) The cullin-RING ubiquitin-protein ligases. *Annu Rev Plant Biol* **62:** 299-334.
26. Callis J (2014) The ubiquitination machinery of the ubiquitin system. *Arabidopsis Book* **12:** e0174.
27. Bueso E *et al.* (2014) The single-subunit RING-type E3 ubiquitin ligase RSL1 targets PYL4 and PYR1 ABA receptors in plasma membrane to modulate abscisic acid signaling. *Plant J* **80:** 1057-1071.
28. Irigoyen ML *et al.* (2014) Targeted degradation of abscisic acid receptors is mediated by the ubiquitin ligase substrate adaptor DDA1 in Arabidopsis. *Plant Cell* **26:** 712-728.
29. Vilela B, Najar E, Lumbreras V, Leung J, Pages M (2015) Casein Kinase 2 Negatively Regulates Abscisic Acid-Activated SnRK2s in the Core Abscisic Acid-Signaling Module. *Mol Plant* **8:** 709-721.
30. Belda-Palazon B *et al.* (2016) FYVE1/FREE1 Interacts with the PYL4 ABA Receptor and Mediates its Delivery to the Vacuolar Degradation Pathway. *Plant Cell* **28:** 2291-2311.
31. Yu F *et al.* (2016) ESCRT-I Component VPS23A Affects ABA Signaling by Recognizing ABA Receptors for Endosomal Degradation. *Mol Plant* **9:** 1570-1582.
32. Yu F, Wu Y, Xie Q (2016) Ubiquitin-Proteasome System in ABA Signaling: From Perception to Action. *Mol Plant* **9:** 21-33.
33. Sheen J (1998) Mutational analysis of protein phosphatase 2C involved in abscisic acid signal transduction in higher plants. *Proc Natl Acad Sci U S A* **95:** 975-980.

34. Kuhn JM, Boisson-Dernier A, Dizon MB, Maktabi MH, Schroeder JI (2006) The protein phosphatase AtPP2CA negatively regulates abscisic acid signal transduction in Arabidopsis, and effects of abh1 on AtPP2CA mRNA. *Plant Physiol* **140:** 127-139.
35. Yoshida T *et al.* (2006) ABA-hypersensitive germination3 encodes a protein phosphatase 2C (AtPP2CA) that strongly regulates abscisic acid signaling during germination among Arabidopsis protein phosphatase 2Cs. *Plant Physiol* **140:** 115-126.
36. Rubio S *et al.* (2009) Triple loss of function of protein phosphatases type 2C leads to partial constitutive response to endogenous abscisic acid. *Plant Physiol* **150:** 1345-1355.
37. Brandt B *et al.* (2015) Calcium specificity signaling mechanisms in abscisic acid signal transduction in Arabidopsis guard cells. *Elife* **4**.
38. Lechner E *et al.* (2011) MATH/BTB CRL3 receptors target the homeodomain-leucine zipper ATHB6 to modulate abscisic acid signaling. *Dev Cell* **21:** 1116-1128.
39. Genschik P, Sumara I, Lechner E (2013) The emerging family of CULLIN3-RING ubiquitin ligases (CRL3s): cellular functions and disease implications. *EMBO J* **32:** 2307-2320.
40. Zhuang M *et al.* (2009) Structures of SPOP-substrate complexes: insights into molecular architectures of BTB-Cul3 ubiquitin ligases. *Mol Cell* **36:** 39-50.
41. Chen L *et al.* (2013) Arabidopsis BPM proteins function as substrate adaptors to a cullin3-based E3 ligase to affect fatty acid metabolism in plants. *Plant Cell* **25:** 2253-2264.
42. Chen L, Bernhardt A, Lee J, Hellmann H (2015) Identification of Arabidopsis MYB56 as a novel substrate for CRL3(BPM) E3 ligases. *Mol Plant* **8:** 242-250.
43. Morimoto K *et al.* (2017) BPM-CUL3 E3 ligase modulates thermotolerance by facilitating negative regulatory domain-mediated degradation of DREB2A in Arabidopsis. *Proc Natl Acad Sci U S A* **114:** E8528-E8536.
44. Zhao Q *et al.* (2013) A plant-specific in vitro ubiquitination analysis system. *Plant J* **74:** 524-533.
45. Wang X *et al.* (2018) ABRE-BINDING FACTORS play a role in the feedback regulation of ABA signaling by mediating rapid ABA induction of ABA co-receptor genes. *New Phytol*. doi: 10.1111/nph.15345
46. Scott DC *et al.* (2016) Two Distinct Types of E3 Ligases Work in Unison to Regulate Substrate Ubiquitylation. *Cell* **166:** 1198-1214.
47. Lu D *et al.* (2011) Direct ubiquitination of pattern recognition receptor FLS2 attenuates plant innate immunity. *Science* **332:** 1439-1442.
48. Li Z, Waadt R, Schroeder JI (2016) Release of GTP Exchange Factor Mediated Down-Regulation of Abscisic Acid Signal Transduction through ABA-Induced Rapid Degradation of RopGEFs. *PLoS Biol* **14:** e1002461.
49. Li Z *et al.* (2018) Abscisic acid-induced degradation of Arabidopsis guanine nucleotide exchange factor requires calcium-dependent protein kinases. *Proc Natl Acad Sci U S A* **115:** E4522-E4531.
50. Moes D, Himmelbach A, Korte A, Haberer G, Grill E (2008) Nuclear localization of the mutant protein phosphatase abi1 is required for insensitivity towards ABA responses in Arabidopsis. *Plant J* **54:** 806-819.
51. Zhu SY *et al.* (2007) Two calcium-dependent protein kinases, CPK4 and CPK11, regulate abscisic acid signal transduction in Arabidopsis. *Plant Cell* **19:** 3019-3036.
52. Lynch T, Erickson BJ, Finkelstein RR (2012) Direct interactions of ABA-insensitive(ABI)-clade protein phosphatase(PP)2Cs with calcium-dependent protein kinases and ABA response element-binding bZIPs may contribute to turning off ABA response. *Plant Mol Biol* **80:** 647-658.

53. Pizzio GA *et al.* (2013) The PYL4 A194T mutant uncovers a key role of PYR1-LIKE4/PROTEIN PHOSPHATASE 2CA interaction for abscisic acid signaling and plant drought resistance. *Plant Physiol* **163:** 441-455.
54. Deblaere R *et al.* (1985) Efficient octopine Ti plasmid-derived vectors for Agrobacterium-mediated gene transfer to plants. *Nucleic Acids Res* **13:** 4777-4788.
55. Clough SJ, Bent AF (1998) Floral dip: a simplified method for Agrobacterium-mediated transformation of Arabidopsis thaliana. *Plant J* **16:** 735-743.
56. Saez A, Rodrigues A, Santiago J, Rubio S, Rodriguez PL (2008) HAB1-SWI3B interaction reveals a link between abscisic acid signaling and putative SWI/SNF chromatin-remodeling complexes in Arabidopsis. *Plant Cell* **20:** 2972-2988.
57. Belda-Palazon B *et al.* (2012) Aminopropyltransferases involved in polyamine biosynthesis localize preferentially in the nucleus of plant cells. *PLoS One* **7:** e46907.
58. Gehl C et al. (2011) Quantitative analysis of dynamic protein-protein interactions in planta by a floated-leaf luciferase complementation imaging (FLuCI) assay using binary Gateway vectors. *Plant J* **67:**542-553.
59. Rodrigues A *et al.* (2013) ABI1 and PP2CA phosphatases are negative regulators of Snf1-related protein kinase1 signaling in Arabidopsis. *Plant Cell* **25:** 3871-3884.
60. Antoni R *et al.* (2012) Selective Inhibition of Clade A Phosphatases Type 2C by PYR/PYL/RCAR Abscisic Acid Receptors. *Plant Physiol* **158:** 970-980.

Figure legends

Fig. 1. BPM3 and BPM5 interact with clade A PP2Cs. (A) Number of PP2CA and BPM peptides identified by IP/Mass Spectrometry (MS). Total proteins were extracted from *$35S_{pro}$:3×FLAG-PP2CA* seedlings treated without (mock) or with ABA and MG132. Immunoprecipitation (IP) was performed using anti-FLAG antibodies and the IP products were analyzed by mass spectrometry. (B) (C) Nuclear interactions of BPM3 or BPM5 with ABI1, ABI2, HAB1 or PP2CA proteins in *N. benthamiana* leaf cells. Confocal images of transiently transformed *N. benthamiana* leaf cells co-expressing either YFP^C-BPM3 (B) or YFP^C-BPM5 (C) and the indicated YFP^N-PP2C protein. Interaction with YFP^N-empty was not observed. Scale bars=10 μm or 40 μm (negative control). (D) Split-LUC complementation assay reveals interaction of BPM3 and BPM5 with PP2CA and HAB1. The indicated construct pairs were coexpressed in *N. benthamiana* leaves (showed in gray) by agrobacterium-mediated infiltration and 50 μM MG132 was applied into the infiltrated region 12 h before measurement of LUC activity, which was performed 60 h after infiltration. LUC activity was measured by applying 1 mM D-luciferin and imaging with a CCD system. LUC signal was converted to false colors with ImageJ and color scale

represents LUC activity. Three independent experiments were performed and images correspond to representative leaves (n=5/each). Histograms indicate quantification of LUC activity that was normalized using co-expression with a GUS expression vector. (E) Y2H interactions of BPM3 and BPM5 with the indicated PP2Cs. Transformed yeast cultures were grown overnight in liquid synthetic defined (SD) medium lacking Leu and Trp and dilutions of these cultures were dropped on either control medium lacking Leu and Trp (SD –LT) or selective medium additionally lacking His (SD –LTH). Empty vectors were used as negative controls and yeasts were allowed to grow for three days at 30°C before interaction was scored.

Fig. 2. Pull-down and coIP experiments show interaction of the indicated BPM and PP2Cs. (A) Pull-down of PP2CA, HAB1, ABI1 and ABI2 with BPM5. His-tagged PP2Cs were incubated with immobilized GST-BPM5 or GST proteins. After washing, proteins were eluted with Laemli buffer and detected by immunoblot analysis using anti-His and anti-GST antibodies**.** The input (1/10 to 1/20) of each His-PP2C added in the experiment and the corresponding PP2C recovered after pull-down (PD) with immobilized GST-BPM5 are indicated. (B) The catalytic PP2CA core is sufficient for interaction with BPM5. His-PP2CA or His-ΔNPP2CA (lacking amino acids 1-99) were incubated with immobilized GST-BPM5 or GST proteins. (C) The MATH domain of BPM5 or BPM3 interacts with PP2CA. His-tagged MATH domain of BPM5 (named MATH5) or BPM3 (named MATH3) was incubated with immobilized GST-PP2CA or GST. (D) Coimmunoprecipitation of the indicated PP2C with HA-BPM5 or HA-BPM3. PP2CA-GFP, GFP-ABI1, GFP-HAB1 or GFP and either HA-BPM5 (top panels) or HA-BPM3 (bottom panels) were coexpressed in *N. benthamiana* leaf cells. Protein extracts were immunoprecipitated (IP) using anti-GFP antibodies. Each immunoprecipitated PP2C was probed with anti-HA antibodies to detect coIP of either HA-BPM5 or HA-BPM3.

Fig. 3. Analysis of BPM3/5-promoted degradation of PP2CA in vivo. (A) In vivo degradation of PP2CA was observed in agroinfiltration experiments with increasing amounts of HA-BPM3 (left) or HA-BPM5 (right) in *N. benthamiana*. The ratio of the relative concentration of agrobacteria used in the different co-infiltrations is indicated by numbers (top). Cell extracts were analyzed using

anti-HA to detect HA-tagged BPM3/5, anti-GFP to detect PP2CA-GFP, and anti-RFP antibodies to detect the internal control of RFP. Molecular masses of marker proteins are indicated in kilodaltons. Asterisk indicates P< 0.05 (Student's t test) when comparing data obtained after 50 μM ABA treatment to those in the absence of exogenous ABA at the same time point. (B) PP2CA protein levels are higher in Col-0 compared to BPM3 or BPM5 OE lines both in mock- or ABA-treated plants. Two-week-old plants grown in liquid MS medium were mock or 50 μM ABA-treated for 3 h and root protein extracts were analyzed using α-E2663 (anti-PP2CA) to detect endogenous PP2CA protein levels. Actin was analyzed as a loading control and numbers indicate average data of the PP2CA signal normalized to Actin in three independent experiments. (C) Higher accumulation of PP2CA after ABA-treatment in Col-0 compared to BPM5 OE lines. Three-week-old plants grown in soil under greenhouse conditions were mock or ABA-sprayed and after 3 h protein extracts from leaves were analyzed using α-E2663 to detect endogenous PP2CA protein levels. Actin was analyzed as a loading control. (D) Enhanced accumulation of PP2CA, HAB1 and ABI1 in the *bpm3 bpm5* double mutant compared to wild type. Root protein extracts were analyzed as described in B. Asterisk indicates P< 0.05 (Student's t test) when comparing data of *bpm3 bpm5* to Col-0 in the same conditions. (E) Degradation of PP2CA is delayed in the *bpm3 bpm5* double mutant compared to wt. Seedlings of Col-0 or bpm3 bpm5 were grown in liquid MS medium for 10 days, and then were supplemented with 50 μM ABA for 3h to induce expression of PP2CA. After ABA washing, 50 μM CHX was added and root samples were harvested at 0, 1, 3 and 6 h. Actin was analyzed as a loading control. Asterisk indicates P< 0.05 (Student's t test) when comparing data of *bpm3 bpm5* to Col-0 at the same time points.

Fig. 4. Overexpression of BPM3 and BPM5 leads to enhanced ABA sensitivity whereas reduced ABA response is found in *amiR-bpm* plants compared to wild-type Col-0. (A) Enhanced sensitivity to ABA-mediated inhibition of seed germination in BPM3 and BPM5 OE lines compared to Col-0 seeds. Approximately 100 seeds of each genotype (two independent experiments) were sown on MS plates lacking or supplemented with 0.5μM ABA. Germination (radicle emergence) was scored after 3d. Values are

averages ± SD. Asterisk indicates P < 0.05 (Student's t test) when comparing data of BPM3 and BPM5 OE lines or the ABA-hypersensitive *hab1-1abi1-2* mutant with Col-0 plants in the same assay conditions. (B) Enhanced sensitivity to ABA-mediated inhibition of seedling establishment. Seedlings were scored for the presence of both green cotyledons and the first pair of true leaves after 8d. Values are averages ± SE. (C) Enhanced sensitivity to ABA-mediated inhibition of root growth in BPM3 and BPM5 OE lines compared to Col-0 plants. Seedlings were grown on MS plates for 4 d and then were transferred to MS plates lacking or supplemented with 10 μM ABA. Root growth was scored after 10 d. Data are means ± SE from three independent experiments (n=20 seedlings per experiment). Asterisk indicates P < 0.05 (Student's t test) when comparing data of BPM3 and BPM5 OE plants with Col-0 plants in the same assay conditions. (D) Diminished water loss in detached leaves of BPM3 and BPM5 OE lines compared to Col-0. Loss of fresh weight was measured in 15-d-old leaves submitted to the drying atmosphere of a laminar flow hood. Asterisk indicates P < 0.05 (Student's t test) when comparing data of BPM3 and BPM5 OE plants with Col-0 plants at the same time points. (E) Enhanced water loss in *amiR-bpm* line compared to Col-0. Loss of fresh weight was measured in detached leaves from 15-d-old plants under laboratory conditions (25ºC, 40% air relative humidity) at the indicated time periods. Asterisk indicates P < 0.05 (Student's t test) when comparing data of *amiR-bpm* with Col-0 plants at the same time points. (F, G) Reduced ABA response in *amiR-bpm* plants compared to Col-0. (F) The course of stomatal conductance (G_{st}) of well-watered plants before and after spraying with 10 μM ABA (n=5 for Col-0 and n=6 for *amiR-bpm*). ABA treatment was done at 14.00 PM and G_{st} followed for the next 6 h. Asterisks indicate significant differences in G_{st} values between *amiR-bpm* and Col-0 at these time points (Student's t-test, P<0.1). SEs are less than 10% and are not indicated for the sake of clarity. (G) ABA-induced reduction in G_{st} of droughted plants, asterisks as before (Student's t-test, P<0.1), n=4 for both lines. (H) ABA-induced stomatal closure of *amiR-bpm* (n=5), *bpm3 bpm5* (n=5) and Col-0 (n=4). Stomatal closure was calculated as pre-treatment stomatal conductance minus stomatal conductance 28 min after ABA spraying. Different letters denote statistically significant differences (ANOVA and Tukey post hoc test).

Fig. 5. Reduced ABA sensitivity of *bpm3 bpm5.* (A) Diminished sensitivity to ABA-mediated inhibition of seedling establishment in *bpm3 bpm5* mutant compared to Col-0. The *pp2ca-1* mutation abolishes the ABA-insensitive phenotype of *bpm3 bpm5* in the triple mutant. Approximately 100 seeds of each genotype were sown on MS plates lacking or supplemented with 1 μM ABA. Seedlings were scored for the presence of both green cotyledons and the first pair of true leaves after 9 d. Asterisk indicates P< 0.05 (Student's t test) when comparing data of *bpm3 bpm5* to Col-0 or *pp2ca-1 bpm3 bpm5* triple to *bpm3 bpm5* double mutant in the same assay conditions. Values are averages of three independent experiments ±SD. (B) Diminished sensitivity to ABA-mediated inhibition of root growth in *bpm3 bpm5* mutant compared to Col-0. Seedlings were grown on MS plates for 4 d and then were transferred to MS plates lacking or supplemented with 10 μM ABA. Root growth was scored after 10 d. Data are means ± SD from three independent experiments (n=20 seedlings per experiment). Asterisk indicates P < 0.05 (Student's t test) when comparing data of *bpm3 bpm5* to Col-0 plants in the same assay conditions. The photographs (right panels) show representative seedlings of the indicated genotypes 10 d after the transfer to MS plates lacking or supplemented with 10 μM ABA. (C) False-color infrared images of Col-0, *bpm3bpm5* and *amiR-bpm* plants representing leaf temperature. Temperature was quantified by infrared thermal imaging. Data are means ±SD (n=5, aprox. 1000 measurements of square pixels from multiple leaves of each plant). (D) Reduced expression of the ABA-responsive markers *RAB18*, *RD29B*, *KIN10* and *RD22* in *bpm3 bpm5* compared to Col-0. RT-qPCR analysis was performed from mRNAs obtained from 2-week-old seedlings. (E) ABA-induced luciferase (LUC) expression driven by *RD29B* promoter was diminished in *bpm3 bpm5* mutant compared to Col-0. Protoplast suspensions were incubated for 6 h after transfection in the absence or presence of 5 μM exogenous ABA added 3 h after transfection. Asterisk indicates P< 0.05 (Student's t test) when comparing data of *bpm3 bpm5* to Col-0 protoplasts in the same conditions. Values are averages ±SD.

Fig. 6. In vivo ubiquitination of PP2CA depends on BPM function. (A) In vivo ubiquitination of PP2CA-GFP in *N. benthamiana*. Agrobacterium encoding PP2CA-GFP was coinfiltrated in leaf cells with agrobacteria lacking (mock) or

co-expressing constitutively HA-BPM3 and β-estradiol-inducible Flag-Ub. Two days after agroinfiltration 1.5 cm disk samples were collected and incubated for 16 h in 100 μM β-estradiol to induce expression of Flag-Ub. Protein extracts were immunoprecipitated using anti-GFP and analyzed by immunoblotting with four different antibodies. (B) Ubiquitination of PP2CA is dependent on BPM function. Arabidopsis seedlings from the indicated genotypes were incubated with MG132 and ABA for 3 h. Total root proteins were incubated with Ub-binding p62 agarose to pull-down ubiquitinated proteins. The α-PP2CA was used to detect non-ubiquitinated and mono-ubiquitinated forms of PP2CA. Actin was analyzed as a loading control. Anti-Ub was used to confirm equivalent recovery of ubiquitinated proteins after pull down (PD) with p62 agarose. Agarose lacking the p62 protein served as a negative control of the experiment. (C) Quantification of PP2CA accumulation in the input samples and the ratio of mono-ubiquitinated versus non-ubiquitinated PP2CA after PD with p62 agarose. Left histogram, the non-ubiquitinated PP2CA protein level in *bpm3 bpm5* and *amiR-bpm* compared to wild-type Col-0; right histogram, the ratio of Ub-PP2CA/non-ubiquitinated PP2CA obtained according to PD p62/Input values, respectively. Asterisk indicates $P < 0.05$ (Student's t test) when comparing data of *bpm3 bpm5* or *amiR-bpm* plants with Col-0 plants in the same assay conditions.

A

protein	IP/MS matching peptides	
	mock IP	ABA+MG132 IP
PP2CA	8	14
BPM3	0	2
BPM4	0	2
BPM5	0	3

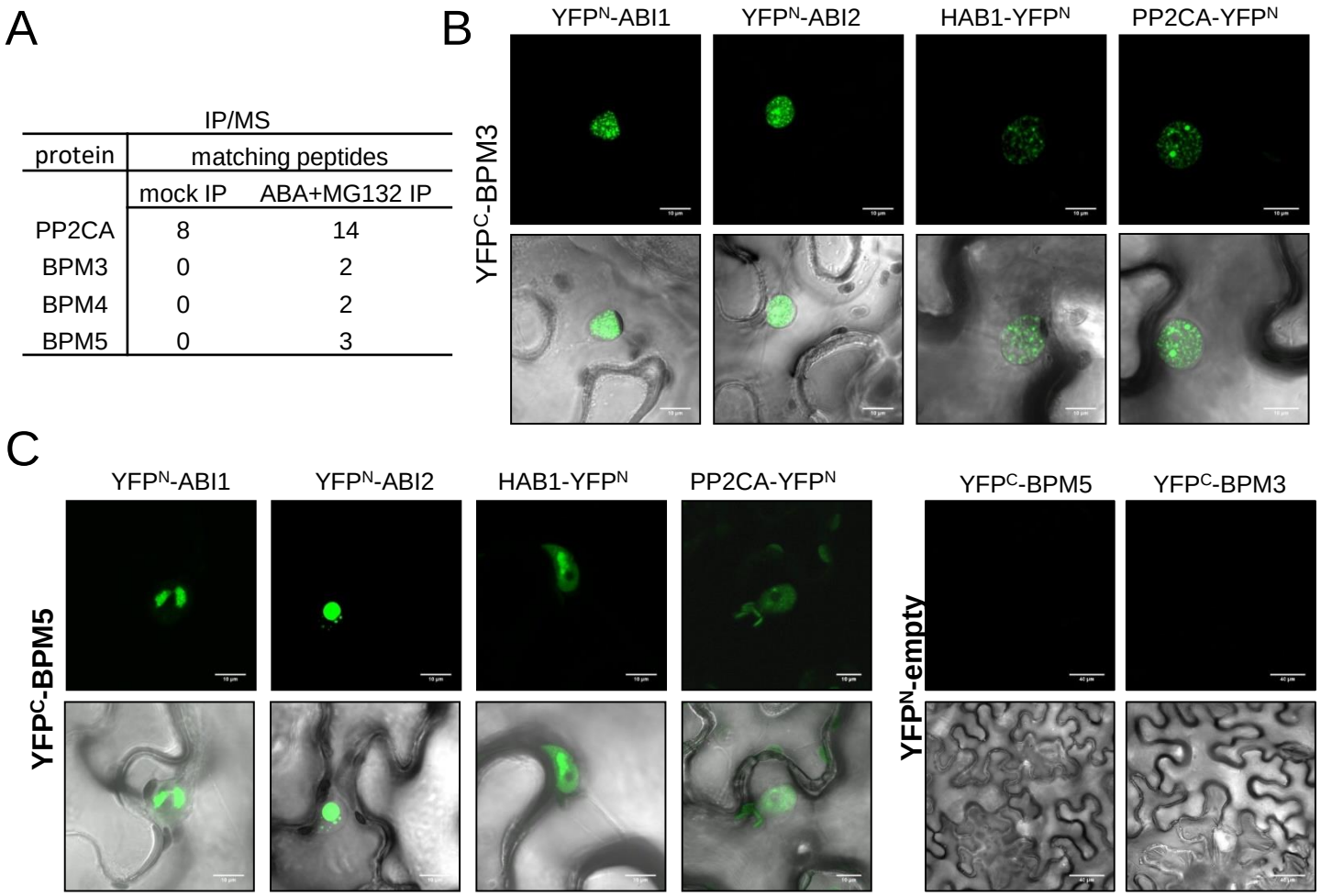

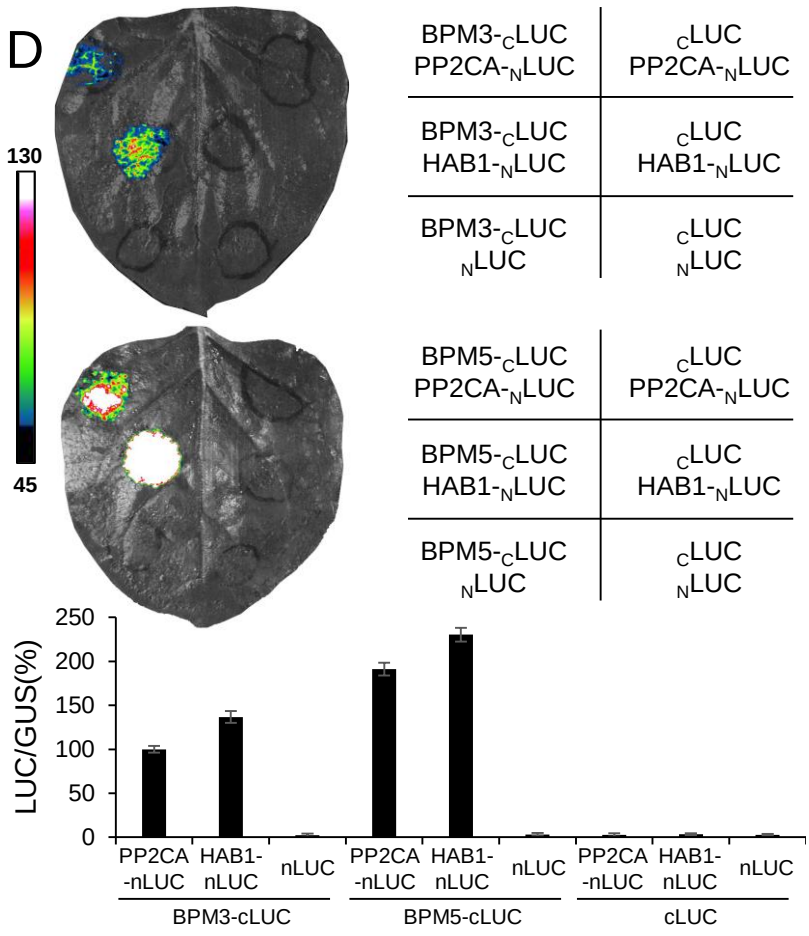

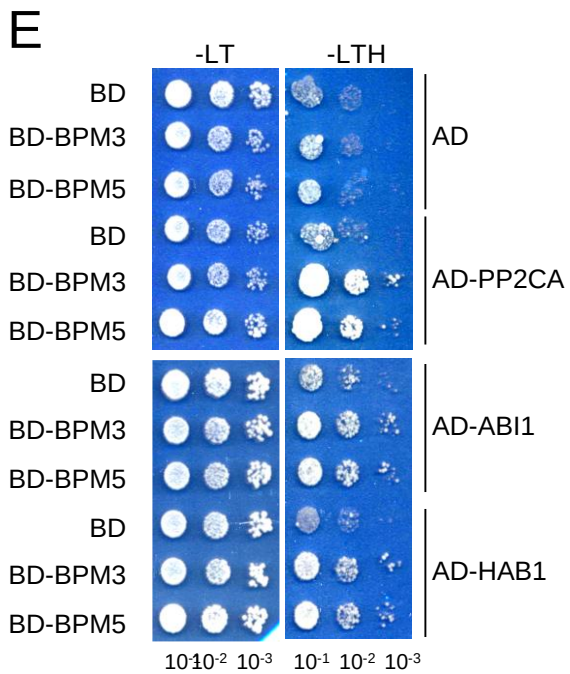

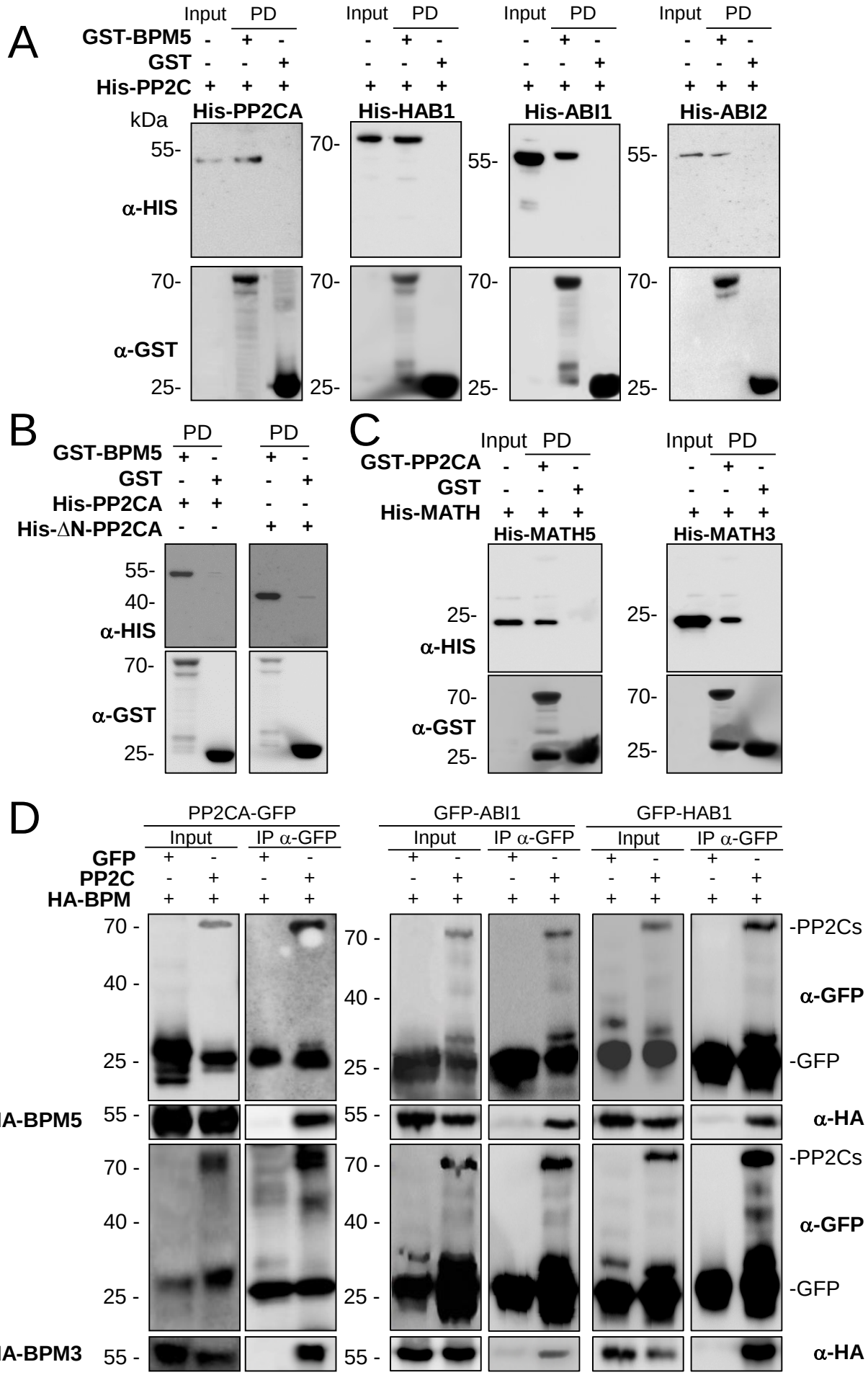
A
Input
PD
GST-BPM5
GST
His-PP2C
His-PP2CA
His-HAB1
His-ABI1
His-ABI2
kDa
55-
70-
25-
α-HIS
α-GST
B
GST-BPM5
GST
His-PP2CA
His-ΔN-PP2CA
55-
40-
70-
25-
α-HIS
α-GST
C
GST-PP2CA
GST
His-MATH
His-MATH5
His-MATH3
25-
70-
α-HIS
α-GST
D
PP2CA-GFP
GFP-ABI1
GFP-HAB1
IP α-GFP
GFP
PP2C
HA-BPM
70 -
40 -
25 -
55 -
-PP2Cs
α-GFP
-GFP
α-HA
HA-BPM5
HA-BPM3

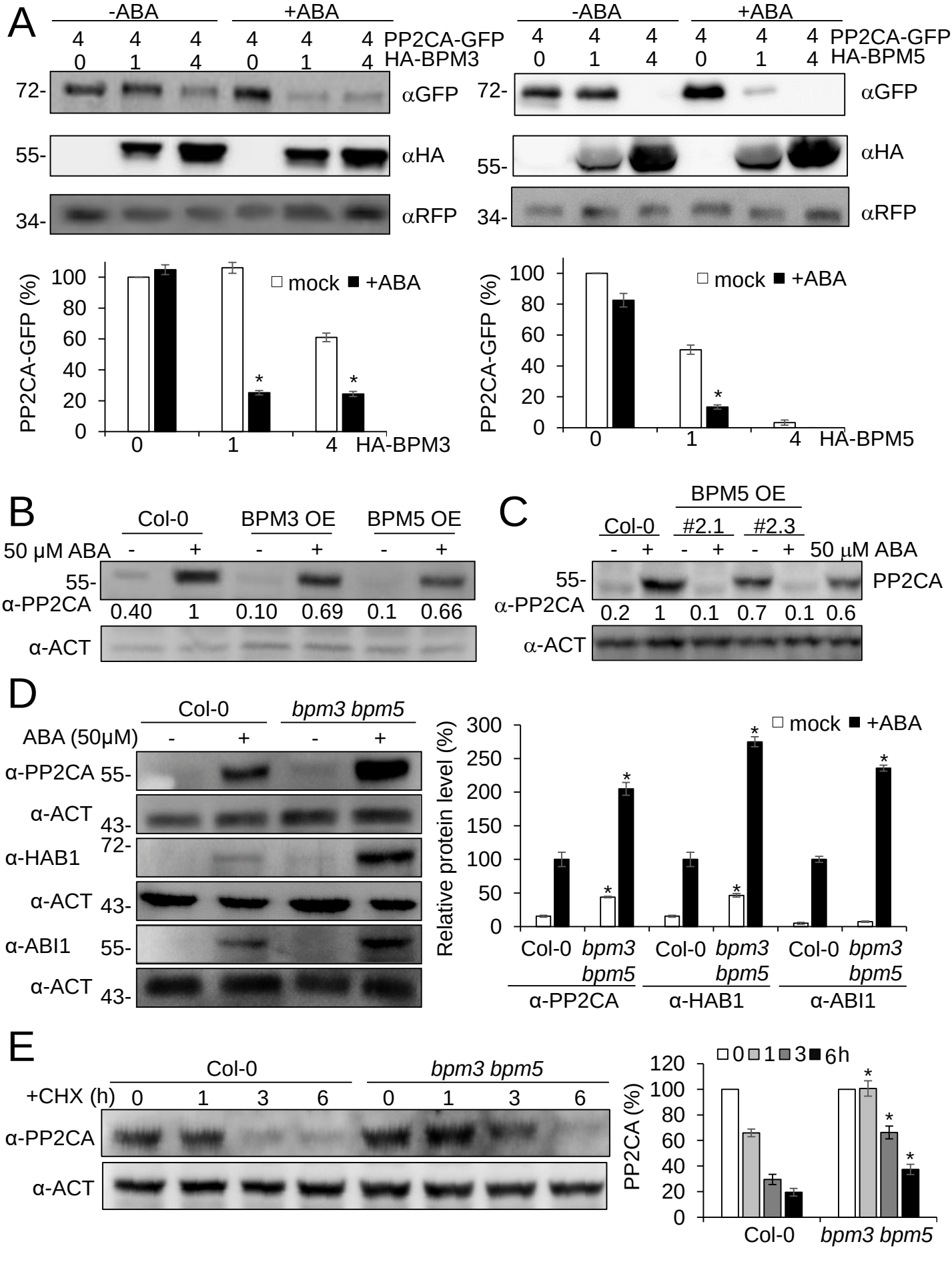
A
-ABA
+ABA
PP2CA-GFP
HA-BPM3
HA-BPM5
αGFP
αHA
αRFP
72-
55-
34-
PP2CA-GFP (%)
mock
+ABA
B
Col-0
BPM3 OE
BPM5 OE
50 μM ABA
α-PP2CA
α-ACT
0.40 1 0.10 0.69 0.1 0.66
C
#2.1
#2.3
0.2 1 0.1 0.7 0.1 0.6
D
bpm3 bpm5
ABA (50μM)
α-HAB1
α-ABI1
Relative protein level (%)
E
+CHX (h)
PP2CA (%)
0 1 3 6h

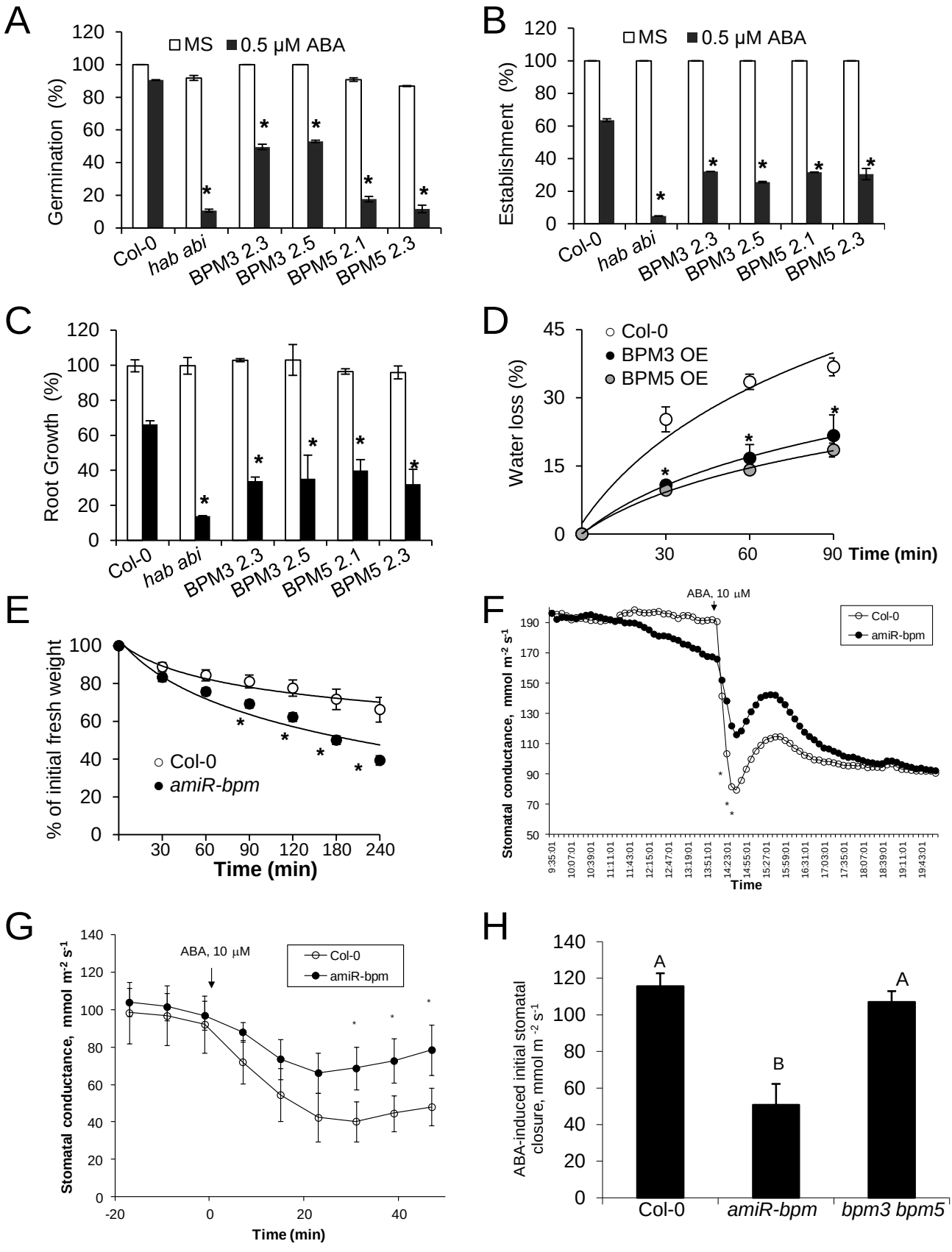
A
MS
0.5 µM ABA
Germination (%)
Col-0
hab abi
BPM3 2.3
BPM3 2.5
BPM5 2.1
BPM5 2.3
B
Establishment (%)
C
Root Growth (%)
D
Col-0
BPM3 OE
BPM5 OE
Water loss (%)
Time (min)
E
% of initial fresh weight
amiR-bpm
Time (min)
F
ABA, 10 µM
Stomatal conductance, mmol m-2 s-1
Time
G
ABA, 10 µM
Time (min)
H
ABA-induced initial stomatal closure, mmol m -2 s-1
A
B
bpm3 bpm5

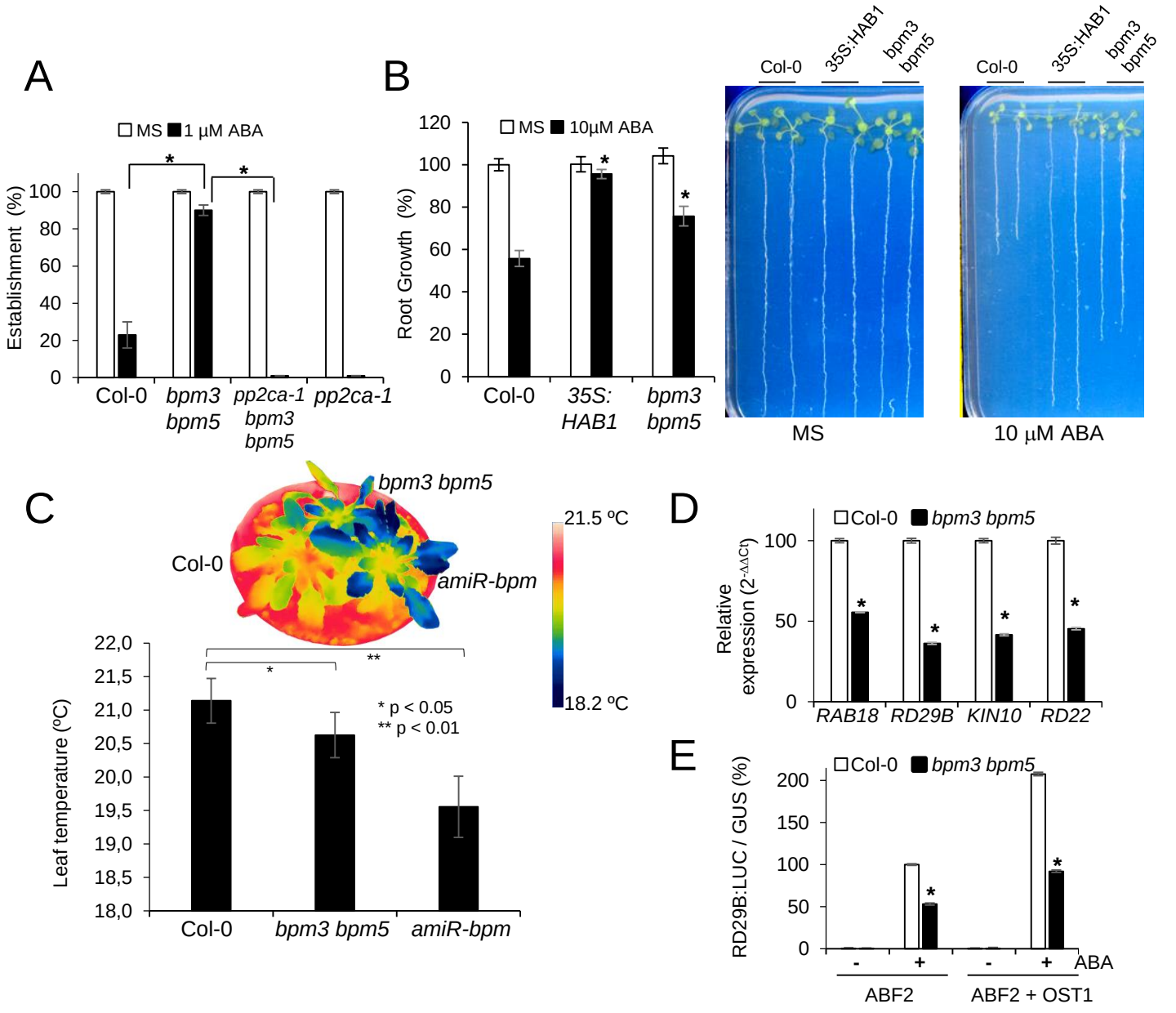
A
MS
1 µM ABA
Establishment (%)
Col-0
bpm3 bpm5
pp2ca-1 bpm3 bpm5
pp2ca-1
B
MS
10µM ABA
Root Growth (%)
Col-0
35S: HAB1
bpm3 bpm5
Col-0
35S:HAB1
bpm3 bpm5
MS
10 µM ABA
C
bpm3 bpm5
Col-0
amiR-bpm
21.5 ºC
18.2 ºC
Leaf temperature (ºC)
* p < 0.05
** p < 0.01
Col-0
bpm3 bpm5
amiR-bpm
D
Col-0
bpm3 bpm5
Relative expression (2-ΔΔCt)
RAB18
RD29B
KIN10
RD22
E
Col-0
bpm3 bpm5
RD29B:LUC / GUS (%)
ABA
ABF2
ABF2 + OST1

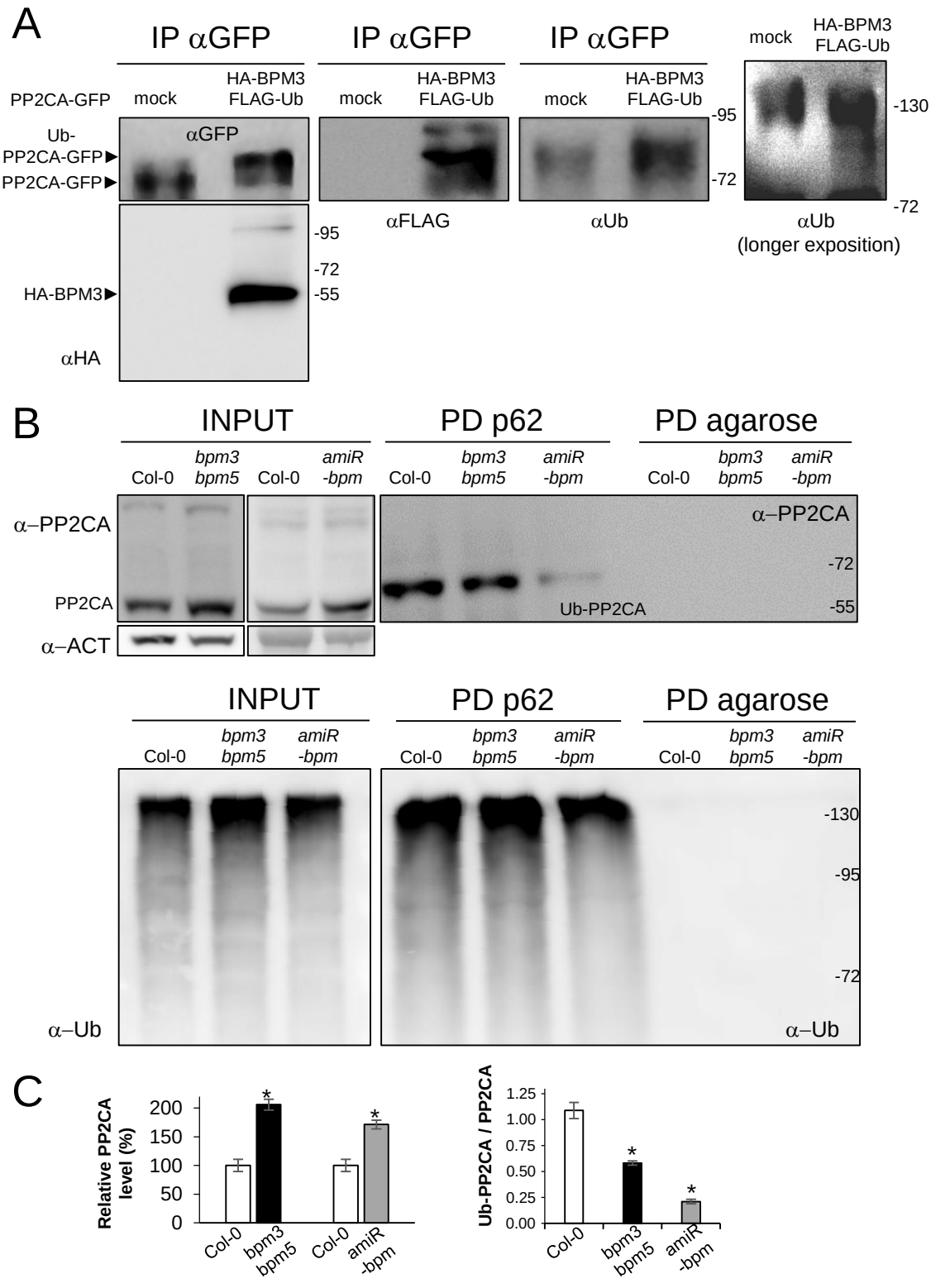
A
IP αGFP
IP αGFP
IP αGFP
mock
HA-BPM3 FLAG-Ub
PP2CA-GFP
Ub-PP2CA-GFP▶
PP2CA-GFP▶
αGFP
αFLAG
αUb
αUb (longer exposition)
HA-BPM3▶
αHA
-95
-72
-55
-130
B
INPUT
PD p62
PD agarose
Col-0
bpm3 bpm5
amiR -bpm
α–PP2CA
PP2CA
α–ACT
Ub-PP2CA
α–Ub
C
Relative PP2CA level (%)
Ub-PP2CA / PP2CA